Mechanisms of Ageing and Development 134 (2013) 391–399

Contents lists available at ScienceDirect

Mechanisms of Ageing and Development

journal homepage: www.elsevier.com/locate/mechagedev

Loss of CB1 receptors leads to decreased cathepsin D levels and accelerated lipofuscin accumulation in the hippocampus

Anastasia Piyanova [a,1], Onder Albayram [a], Carlo Alberto Rossi [b], Hany Farwanah [c], Kerstin Michel [a], Pierluigi Nicotera [b], Konrad Sandhoff [c], Andras Bilkei-Gorzo [a,*]

[a] Institute of Molecular Psychiatry, University of Bonn, Sigmund-Freud-Straße 25, 53127 Bonn, Germany
[b] Deutsches Zentrum für Neurodegenerative Erkrankungen (DZNE), Ludwig-Erhard-Allee 2, 53175 Bonn, Germany
[c] Life and Medical Sciences (LIMES), Membrane Biology and Lipid Biochemistry Unit, University of Bonn, c/o Kekulé-Institut für Organische Chemie und Biochemie der Universität, Gerhard-Domagk-Str. 1, 53121 Bonn, Germany

ARTICLE INFO

Article history:
Received 8 May 2013
Received in revised form 10 July 2013
Accepted 3 August 2013
Available online 13 August 2013

Keywords:
Endocannabinoid system
Hippocampus
Oxidative stress
LC3
p62
Autophagy

ABSTRACT

Early onset of age-related changes in the brain of cannabinoid 1 receptor knockout ($Cnr1^{-/-}$) mice suggests that cannabinoid 1 (CB1) receptor activity significantly influences the progression of brain aging. In the present study we show that lack of CB1 receptors leads to a significant increase in lipofuscin accumulation and a reduced expression and activity of cathepsin D, lysosomal protease implicated in the degradation of damaged macromolecules, in the hippocampus of 12-month-old mice. The impaired clearance of damaged macromolecules due to the low cathepsin D levels and not enhanced oxidative stress may be responsible for the lipofuscin accumulation because macromolecule oxidation levels were comparable between the genotypes within the same age group. The altered levels of autophagy markers p62 and LC3-II suggest that autophagy is upregulated in CB1 knockout mice. Increased autophagic flux in the absence of CB1 receptors is probably a compensatory mechanism to partially counteract decreased lysosomal degradation capacity. Together, these results suggest that CB1 receptor activity affects lysosomal activity, degradation of damaged macromolecules and thus it may influence the course and onset of brain aging.

1. Introduction

Aging of the brain is one of the major risk factors for neurodegeneration and cognitive decline (Bishop et al., 2010). It has been recently suggested that the endocannabinoid system protects against negative consequences of brain aging, such as neuroinflammation, neuronal loss and cognitive deficits (Albayram et al., 2011). The endocannabinoid system comprises the cannabinoid receptors – CB1 (highly expressed in the central nervous system) and CB2 (preferentially expressed on immune cells), their endogenous ligands (anandamide, AEA, and 2-arachidonoylglycerol, 2-AG) and the enzymes involved in the synthesis and degradation of the endocannabinoids (Di Marzo et al., 2004). Mice lacking CB1 receptors show symptoms of accelerated ageing, including early loss of subdermal fat, memory deficits (Albayram et al., 2012; Bilkei-Gorzo et al., 2005), neuronal loss and increased neuroinflammation (Albayram et al., 2011). Interestingly, neuronal loss and changes in the inflammatory profile were restricted to the hippocampus: other brain regions like striatum or cortex, which are also known for high CB1 receptor density, were not affected (Albayram et al., 2011). The onset of microglia activation was determined to be at the age of 12 months, whereas learning impairments and pyramidal cell loss preceded it (Albayram et al., 2011; Bilkei-Gorzo et al., 2005, 2012). Thus, regulation of neuroinflammatory processes is not the only mechanism by which CB1 receptor activity influences the course of brain aging. A possible trigger of neuroinflammation is the increased concentration of damaged macromolecules and protein aggregates as a result of a disturbed balance between their generation and clearance. Aging is generally accompanied by an increase in oxidative stress (Golden et al., 2002; Harman, 1956), as well as by mitochondrial dysfunction (Hekimi and Guarente, 2003; Sastre et al., 2003) leading to increased generation of reactive oxygen species (ROS). Moreover, protein degradation machinery and quality control systems become significantly impaired with increasing age, leading to the accumulation of degradation end products, such as lipofuscin (Nakanishi et al.,

* Corresponding author at: Institute of Molecular Psychiatry, c/o Life & Brain Center, University of Bonn, Sigmund-Freud-Straße 25, 53127 Bonn, Germany. Tel.: +49 2286885317; fax: +49 6885301.
E-mail address: abilkei@uni-bonn.de (A. Bilkei-Gorzo).
[1] Present address: Deutsches Zentrum für Neurodegenerative Erkrankungen (DZNE), Ludwig-Erhard-Allee 2, 53175 Bonn, Germany.

0047-6374/$ – see front matter © 2013 Elsevier Ireland Ltd. All rights reserved.
http://dx.doi.org/10.1016/j.mad.2013.08.001

1997). Lipofuscin is a lipopigment, which consists of aggregated products of lysosomal degradation, including oxidized and misfolded proteins, lipids, defective mitochondria and metal ions, particularly iron (Dunlop et al., 2009; Terman and Brunk, 2004). Enhanced accumulation of lipofuscin could be a result of increased oxidative damage, autophagy deficits and altered lysosomal degradation process (Brunk and Terman, 2002). The latter can be attributed to a loss-of-function of specific lysosomal proteases, such as cathepsin D (Koike et al., 2000). A knockout of cathepsin D in mice causes symptoms similar to those typical for neuronal ceroid lipofuscinoses in humans–a massive accumulation of autofluorescent pigment (ceroid/lipofuscin) in the brain and decreased lifespan (Koike et al., 2000; Nakanishi et al., 2001; Walls et al., 2007). Massive neurodegeneration occurring in cathepsin D deficient mice has been attributed to microglia activation (Yamasaki et al., 2007). Cathepsin D expression and intracellular distribution are also known to be affected by aging (Nakanishi, 2003). Although lipofuscin accumulation is often considered to be just an aging marker, many studies have shown that it often accompanies cellular degeneration and inflammatory processes (Cai et al., 2012; Ma et al., 2013; Shiozaki et al., 2008), as well as cognitive decline during aging (Kadar et al., 1990). Lipofuscin is considered to be the major source of oxidants in aging cells (Hohn et al., 2010). The presence of lipofuscin can also influence important cellular processes, such as autophagy, by inhibiting the fusion between autophagosomes and lysosomes, thus further exacerbating the accumulation of degradation products in the cell.

In this study we show that the lack of CB1 receptors exacerbates age-related lipofuscin accumulation in the hippocampus, but not other brain areas, also known to have a high CB1 receptor density (Lutz, 2002). This finding is in line with our previous studies showing that hippocampus is the area most vulnerable to CB1 receptor deletion (Albayram et al., 2011). Since the endocannabinoid system has previously been implicated in antioxidative defence (Kim et al., 2005), we first assessed oxidative damage to proteins, lipids and DNA in the brains of wildtype ($Cnr1^{+/+}$) and CB1 knockout ($Cnr1^{-/-}$) mice. We found that the lack of CB1 receptors does not lead to increased oxidative stress during aging. We then hypothesized that the clearance of damaged macromolecules is the reason for increased accumulation of lipofuscin. We found a significant decrease in the protein levels of all cathepsin D isoforms, as well as reduced cathepsin D activity in CB1 knockout mice, which could potentially be responsible for lipofuscin accumulation. We have also shown that autophagy is upregulated in $Cnr1^{-/-}$ mice, which is probably a compensatory reaction to the reduced lysosomal degradation capacity. These changes were not accompanied by disturbances in the mTOR pathway. In summary, lack of CB1 receptors leads to a progressive increase in lipofuscin accumulation specifically in the hippocampal region, which may contribute to accelerated brain ageing.

2. Materials and methods

2.1. Animals

Young (2–3 month-old) and old (12–15-month-old) male and female $Cnr1^{+/+}$ and $Cnr1^{-/-}$ mice were derived from a heterozygous $Cnr1^{+/-}$ breeding colony on a congenic C57BL/6J background maintained in the House of Experimental Therapy, University of Bonn. Mice received food and water *ad libitum*, were housed as single sex littermates in groups of 2–5 and were kept on a reversed light-dark cycle (dark period between 9 am and 7 pm). Animal care and conduction of experiments followed the guidelines of the 1998 German Animal Protection Law.

2.2. Tissue preparation

Male and female animals of both age groups and genotypes were sacrificed by CO_2 inhalation, decapitated and their brains were isolated. Brains for the histological determination of lipofuscin and oxidized DNA content were snap frozen in dry ice cooled isopentane and stored in −80 °C until further processing. Next, frozen brain was serially sliced in 18 μm coronal slices in a Cryostat (Leica CM 3050; Leica Microsystems, Heidelberg, Germany) and mounted onto silanized glass slides.

Hippocampus, striatum and cortex for the determination of oxidized protein and lipid levels, as well as for Western blot analysis were quickly isolated from the brain using the punch technique. The individual areas were identified by the anatomical boundaries using the mouse brain atlas (Paxinos and Franklin, 2001). Isolated brain areas were shock frozen and kept at −80 °C until further processing.

2.3. Cell culture

Primary cultures of hippocampal neurons were prepared from E17.5 embryos of $Cnr1^{+/+}$ and $Cnr1^{-/-}$ mice in sterile HIB buffer (120 mM NaCl, 5 mM KCl, 25 mM HEPES, pH 7.4) supplemented with 9.1 mM glucose, followed by trypsin digestion for 10 min at 37 °C. Cells were then pelleted by centrifugation, resuspended in pre-plating medium (Neurobasal medium with 1% penicillin/streptomycin, 0.5 mM glutamine, 5% FBS and 2% B27 supplement; Life Technologies), plated in droplets onto poly-L-lysine and laminin coated plates and allowed to attach for 1–2 h, after which 1 ml of Pre-Plating Medium was added. AraC (1:1000) in plating medium (without FBS) was added to the cells 24 h after plating to inhibit the proliferation of glial cells. 48 h after plating half of the medium was replaced with fresh plating medium, and this procedure was repeated every 2–3 days. Cells were treated with rapamycin (0.2 μM) and bafilomycin A_1 (20 nM) for 24 h and collected for Western Blot analysis on 14DIV.

2.4. Determination of lipofuscin accumulation in the hippocampus by autofluorescence

Two-three animals were used from each genotype, sex and age group to assess lipofuscin levels. Sections from the frozen brains were postfixed in 4% paraformaldehyde in phosphate buffered saline (PBS), washed with TBS and slides were covered using Vectashield mounting medium for fluorescence (Vector Laboratories Inc., Burlingame, CA) containing 4′,6-diamidino-2-phenylindole (DAPI). Section images were acquired using the Leica TCS SP8 confocal microscope system. Images were analysed using ImageJ software (National Institute of Mental Health, Bethesda, Maryland, USA). Lipofuscin level was measured as the presence of lipofuscin-like autofluorescence at 500–550 nm in the region of interest. For quantification pictures were converted to 8-bit grey scale and the mean signal intensities within the CA3 region were determined using the ImageJ software. For statistical analysis three-four representative slides were evaluated from each animal. Groups were compared using two-way ANOVA (main factors: age and genotype) followed by Bonferroni test. Data are presented as mean values of fluorescence intensity.

2.5. Lipid peroxidation determination

Lipid peroxidation was assessed by measuring the presence of thiobarbituric acid reactive substances (TBARS) in the total hippocampus homogenates of $Cnr1^{+/+}$ and $Cnr1^{-/-}$ mice as described previously (Bruce and Baudry, 1995). The probes were homogenized in 50 mM phosphate buffer pH 7.4 (PBS) in the presence of deferoxamine. Equal volumes of homogenates were added to an aqueous solution containing acetic acid and thiobarbituric acid. An aliquot was also taken for protein content determination. After heating this mixture to 95 °C for 1 h a 1-butanol/pyridine solution was added, and TBARS were extracted into the organic layer by centrifugation at 4000 × *g* for 10 min. The amounts of TBARS were determined by spectrophotometry at 532 nm on an Ultrospec 2100 *pro* UV–vis spectrophotometer (GE Healthcare, Freiburg, Germany) and calculated as nmol malondialdehyde equivalent per μg of protein according to a standard curve prepared from malondialdehyde bis-dimethyl acetal.

2.6. Protein carbonylation determination

Protein carbonyl content, as an index of protein oxidation, was measured by the 2,4-dinitrophenylhydrazine (DNPH) method, as described in the literature (Dubey et al., 1996; Levine, 2002; Levine et al., 1994; Reznick and Packer, 1994). For each sample, the supernatants were divided into two equal volumes–test probe (with DNPH) and blank (without DNPH). Samples were then incubated for 1 h at room temperature in the dark with continuous stirring and precipitated with equal volumes of 20% trichloroacetic acid (TCA) for 10 min on ice, centrifuged at 3000 × *g* for 5 min, and supernatants were discarded. Protein pellets were washed in ethanol/ethyl acetate (1:1) mixture for three times to remove free DNPH and additional lipid contaminants. Final protein precipitates were dissolved in 6 M guanidine hydrochloride solution. The carbonyl content of both test and control samples was determined by spectrophotometry at 370 nm using molar extinction coefficient and expressed as nmol carbonyl per mg of soluble extracted protein.

2.7. Immunohistochemical staining for oxidized DNA

Immunohistochemical staining to detect oxidative damage to DNA was performed using standard procedures. Briefly, frozen brains were cut into 16 μm sections using a cryostat (Leica CM 3050, Leica Microsystems). Sections were postfixed in 4% paraformaldehyde in phosphate buffered saline (PBS), washed

with TBS, permeabilized with 0.2% Triton-X 100 in TBS, and then antigene retrieval was performed using citrate buffer, pH 6. Sections were then washed and blocked with 10% donkey serum/TBS and then additionally blocked to prevent unspecific binding of primary antibody developed in mouse using Mouse On Mouse Blocking Kit (Vector Laboratories, Inc., Burlingame, CA), followed by incubation with the monoclonal mouse anti-8-hydroxyguanosine antibody diluted 1:1000 (Abnova, Heidelberg, Germany) overnight. Sections incubated with 10% donkey serum/TBS without primary antibody were used as negative controls and were provided on each slide. Additionally, we used RNase A treated samples, as controls for specificity of anti-8-hydroxyguanosine antibody for DNA as previously described (Strazielle et al., 2009). On the next day, sections were washed with TBS and then incubated with Alexa fluor 647-coupled secondary antibody (Invitrogen, Carlsbad, CA). After the incubation, sections were washed and covered with Vectashield mounting medium for fluorescence (Vector Laboratories Inc., Burlingame, CA) containing 4′,6-diamidino-2-phenylindole (DAPI) for counterstaining. Section images were acquired using an immunofluorescence microscope (Zeiss, Axioplan 2 imaging) connected to a digital camera (Zeiss) and a PC system with AxioVision imaging software. Images were analysed using ImageJ software (National Institute of Mental Health, Bethesda, MD, USA). Data are presented as mean values of staining intensity per total area.

2.8. Western blots

Hippocampi from $Cnr1^{+/+}$ and $Cnr1^{-/-}$ mice were sonicated in RIPA buffer or 1% SDS (for LC3 blots) containing protease inhibitors. Protein content was determined using a commercially available bicinchoninic acid (BCA) assay kit from Pierce (Thermo Scientific, Rockford, IL). The absorbance was measured at 570 nm on a Revelation Microtiter Plate Reader (Dynex Technologies MRX-TC). Protein concentration was calculated from the optical density values according to the standard curve of bovine serum albumine. 20–30 μg of total protein was then used for Western blot analys. Cell culture samples (200,000 cells per well) were directly lysed in Laemmli buffer. The samples were run on polyacrylamide gels, blotted onto nitrocellulose membranes and subsequently probed with primary antibodies to LC3 (1:500; Sigma), p62/SQSTM1 (1:500; Progen), cathepsin D (1:1000; Santa Cruz), LAMP1 (1:500, Millipore), phospho-mTOR Ser2448 (1:500, Cell Signaling), mTOR (1:500, Abcam), ß-actin (1:10,000; Sigma), α-tubulin (1:5000, Sigma). Blots were then incubated with peroxidase-conjugated secondary antibodies, and positive signals were detected using chemiluminescent substrates of peroxidase (ECL, Pierce). Quantification was performed using the ChemiDoc software (BioRad). Cathepsin D blots were exposed using high performance autoradiography film (Amersham Hyperfilm® MP, GE Healthcare, Buckinghamshire, UK) and developed using CP 1000 AGFA Healthcare N.V. film developer. The films were then scanned using Epson Perfection 4990 scanner and analysed using ImageJ software.

2.9. Cathepsin D activity in the hippocampus

$Cnr1^{+/+}$ and $Cnr1^{-/-}$ mice ($n = 6$ per group) were killed by cervical dislocation, hippocampi were quickly isolated and homogenized in ice-cold PBS using hand dounce homogenizer. After removing the nuclear fraction and cell debri by centrifugation (10 min at 600 × g), the supernatant was centrifuged again for 5 minutes at 20,000 × g to recover the lysosomal fraction, which was then re-suspended in ice-cold PBS. Cathepsin D activity was measured using the Cathepsin D assay kit (Sigma, Saint Luis, USA). Enzyme activity was assessed by the time-dependent increase in the fluorescence of 7-methoxycoumarin (MCA), product of cathepsin D activity. The fluorescence was measured in a microplate reader (Infinite M200 Pro, Tecan, Austria). To control the specificity of the reaction to cathepsin D, changes in MCA fluorescence were measured in the presence of the enzyme blocker pepstatin. Protein content of the lysosomal fraction was determined using BCA protein assay kit (Thermo Scientific, Rockford, USA). Enzyme activity was calculated as nmol MCA produced per mg protein.

2.10. Lipid extraction, densitometric quantification and mass spectrometric profiling of ceramide species

Frozen mouse hippocampi were homogenized in milliQ water using an Ultra-Turrex® homogenizer (IKA Werke, Staufen, Germany). To ensure maximal lipid yield, sequential extractions starting with chloroform, methanol, water (1:2:0.8; V/V/V) followed by chloroform, methanol (1:1; V/V), and ending with chloroform, methanol (2:1, V/V) were performed. The extraction steps were carried out overnight at 40 °C in a water bath. Afterwards, the extracts were pooled, and the solvents evaporated under a stream of nitrogen. Further processing was performed as described previously elsewhere (Farwanah et al., 2009). However, no alkaline hydrolysis was conducted. For quantification purposes, lipid extracts were initially applied onto silica HPTLC (Merck, Darmstadt, Germany) plates using Linomat® 4 (CAMAG, Berlin, Germany). The lipids were then separated by developing the plates twice in a horizontal chamber (CAMAG, Berlin, Germany) using a solvent mixture consisting of chloroform, methanol and acetic acid (190:10:1; V/V/V). The separated bands were visualized by dipping the plates into a solution of 10% $CuSO_4$ and 8% H_3PO_4 (w/v) and subsequently heating them on a TLC plate heater (CAMAG, Berlin, Germany) at 180 °C for 15 min. The quantification was performed densitometrically using a TLC scanner 3 (CAMAG, Berlin, Germay) by relating the detected intensities to a previously comprised standard curve (Farwanah et al., 2009). The profiling of the ceramide species was carried out using an LC/ESI-QTOF-MS method as described elsewhere (Farwanah et al., 2011).

2.11. Real-time PCR analysis

Total RNA was extracted using the TRIzol® reagent (Invitrogen, Life Technologies) according to manufacturer's instructions and transcripted to cDNA using the SuperScript First-Strand Synthesis System for RT-PCR Kit (Invitrogen Corp., Carlsbad, CA, USA). Differences in mRNA expression were determined as described previously (Albayram et al., 2011) by custom TaqMan® Gene Expression Assays (Applied Biosystems, Darmstadt, Germany) for cathepsin D (Mm00515586_m1) and p62/SQSTM1 (Mm00500417_m1) with glyceraldehyde-3-phosphate dehydrogenase (GAPDH) as a control to standardize the amount of target cDNA. Samples were processed in a 7500 Real-Time PCR Detection System (Applied Biosystems, Darmstadt, Germany), and further analysis was performed using the 7500 Sequence Detection Software version 2.2.2 (Applied Biosystems, Darmstadt, Germany). Data are presented as $2^{-\Delta\Delta Ct}$ (Livak and Schmittgen, 2001)

2.12. Statistical analysis

Statistical analysis was performed using GraphPad Prizm (Version 4.0) software and STATISTICA Version 6.0. Age- and genotype-related changes were analysed using two-way ANOVA (main factors: age, genotype) and three-way ANOVA (main factors: age, genotype, sex) followed by Bonferroni's *post hoc* tests. Data are represented as mean values (+/− standard error of mean).

3. Results

3.1. Enhanced lipofuscin accumulation in the hippocampus, but not in other brain regions, of CB1 knockout mice

We compared the intensity of lipofuscin autofluorescence in the cortex, striatum and CA3 area of the hippocampus in young (2–3 months old) and old (12–15 month-old) $Cnr1^{+/+}$ and $Cnr1^{-/-}$ mice. There was an age-related increase in lipofuscin autofluorescence in each of the brain areas tested (cortex: $F_{1,108} = 50.33$, $p < 0.001$; striatum $F_{1,104} = 23.48$, $p < 0.001$; hippocampus: $F_{1,68} = 216.9$, $p < 0.001$ Fig. 1A and Supplementary Fig. 1A and B). The accumulation of lipofuscin was significantly exacerbated in the hippocampus of $Cnr1^{-/-}$ mice at 12–15 months of age, as compared to the age-matched wildtype mice (genotype effect: $F_{1,68} = 8.827$, $p < 0.01$; age × genotype interaction effect: $F_{1,68} = 18.93$, $p < 0.001$). Additionally, we found no difference in lipofuscin accumulation in aging between male and female specimens in the examined areas in independent samples (data not shown), except the cortex, where lipofuscin accumulation was higher in the females (sex × age: $F_{1,104} = 9.262$, $p < 0.01$; Supplementary Fig. 2); this effect was present in both genotypes.

Supplementary material related to this article can be found, in the online version, at http://dx.doi.org/10.1016/j.mad.2013.08.001.

3.2. The amount of oxidized macromolecules in the brain increases with age independently of the presence of the CB1 receptor

To test whether oxidative stress contributes to the exacerbated lipofuscin accumulation in the hippocampus of $Cnr1^{-/-}$ mice, we compared the amount of oxidized macromolecules in young and old $Cnr1^{+/+}$ and $Cnr1^{-/-}$ mice. The amount of peroxidized lipids, assessed as the concentration of thiobarbituric acid-reactive substances (TBARS), did not show significant differences between the age groups (age effect: $F_{1,18} = 0.036$, $p > 0.05$) and genotypes (genotype effect: $F_{1,18} = 0.212$, $p > 0.05$; Fig. 2A) in the hippocampus. Additionally, we assessed the amount of peroxidized lipids in cortex and striatum, where lipofuscin load was similar between the genotypes: there was no difference in lipid oxidation between age groups or genotypes in the cortex (age effect: $F_{1,17} = 2.853$, $p > 0.05$; genotype effect: $F_{1,17} = 0.283$, $p > 0.05$; Supplementary Fig. 3A) and striatum (age effect: $F_{1,16} = 0.861$, $p > 0.05$; genotype

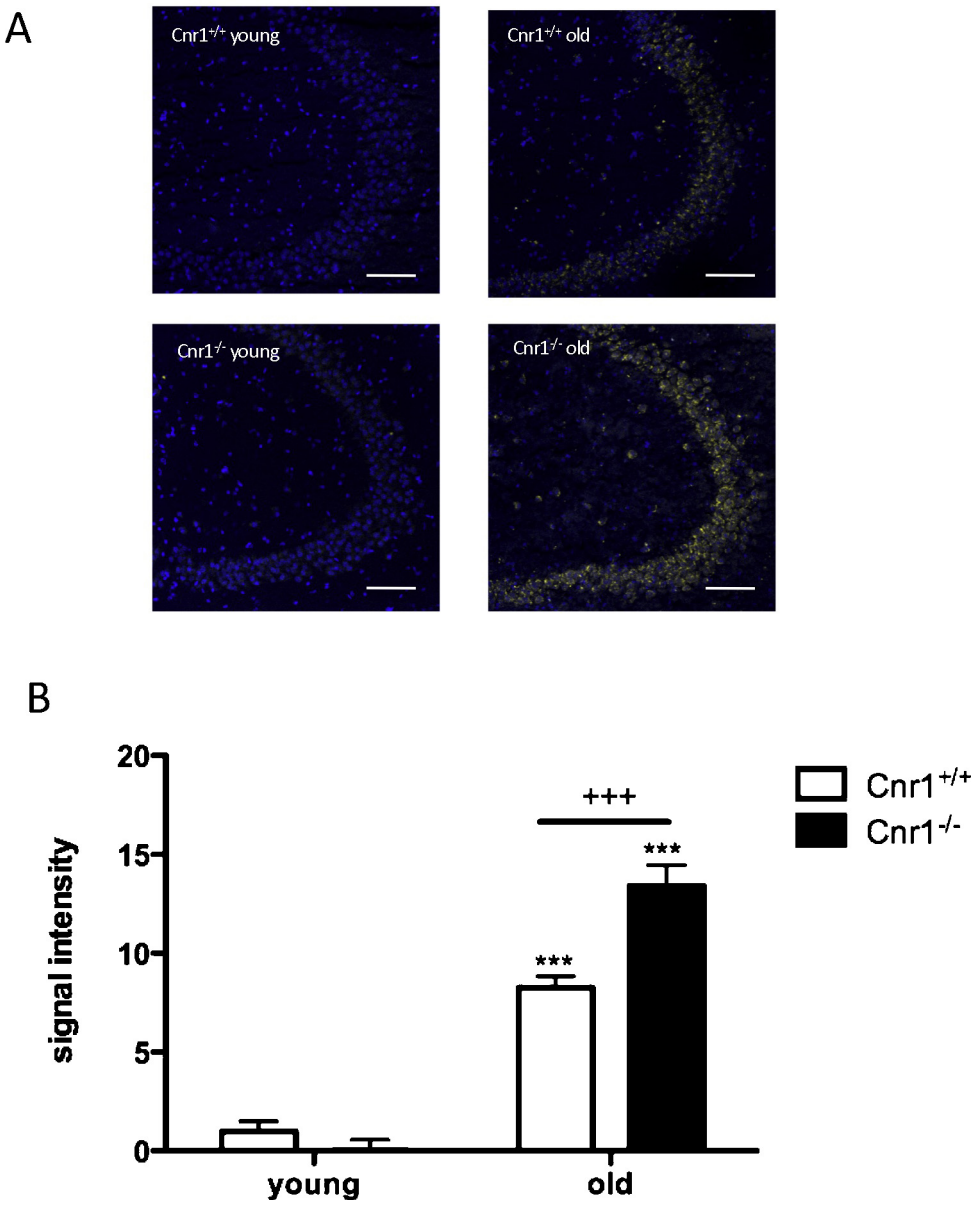

Fig. 1. Increased lipofuscin accumulation in the CA3 region of the hippocampus in aged CB1 knockout mice. (A) Representative confocal microscopy images of the CA3 region of the hippocampus in young and old wild type ($Cnr1^{+/+}$) and CB1 receptor knockout ($Cnr1^{-/-}$) mice. Brain slices were stained with 4′,6-diamidino-2-phenylindole (DAPI) to visualize the nuclei of the cells (blue fluorescence). Lipofuscin accumulation is indicated by the presence of yellowish autofluorescence (number of slices evaluated per group = 18). Scale bar: 100 μm. (B) Quantification of lipofuscin autofluorescence in the CA3 region of the hippocampus in young and old $Cnr1^{+/+}$ and $Cnr1^{-/-}$ mice. Columns represent group mean values; error bars represent standard errors of mean (SEM). $^{+++}p < 0.001$ difference between the genotypes within the same age group; $^{***}p < 0.001$ difference between the age groups, both Bonferroni's *post hoc* test. (For interpretation of the references to color in this figure legend, the reader is referred to the web version of this article.)

effect: $F_{1,16} = 2.224$, $p > 0.05$; Supplementary Fig. 3B). Oxidative damage to proteins was assessed as the concentration of carbonyl groups. Protein carbonylation in the hippocampus was found to increase with age (Fig. 2B; age effect: $F_{1,23} = 26.14$, $p < 0.001$), similarly in both genotypes (genotype effect: $F_{1,23} = 1.786$, $p > 0.05$; interaction: $F_{1,23} = 1.334$). Cortex (age effect: $F_{1,19} = 2.515$, $p > 0.05$; genotype effect: $F_{1,19} = 0.213$, $p > 0.05$; interaction: $F_{1,19} = 0.296$, $p > 0.05$; Supplementary Fig. 3C) and striatum (age effect: $F_{1,18} = 0.203$, $p > 0.05$; genotype effect: $F_{1,18} = 0.212$, $p > 0.05$; interaction: $F_{1,18} = 0.054$, $p > 0.05$; Supplementary Fig. 3D) showed no signs of increased protein oxidation up to the age of 12–15 months in both genotypes. Oxidative damage to total DNA was assessed as the intensity of 8-hydroxyguanosine-specific staining in cortex, striatum and the CA3 region of the hippocampus. There was a significant increase in the amount of oxidized DNA in aging in the hippocampus (Fig. 2C; age effect: $F_{1,55} = 59.68$, $p < 0.001$), however, no genotype effect (genotype effect: $F_{1,55} = 0.086$, $p > 0.05$) or interaction ($F_{2,55} = 0.063$, $p > 0.05$) was observed. The effect was similar between males and females (data not shown). In the cortex we found a similar phenomenon: there was a significant difference between the age groups ($F_{1,106} = 51.47$, $p < 0.001$; Supplementary Fig. 4A), whereas no genotype effect or genotype × sex interaction was present (genotype effect: $F_{1,106} = 2.983$, $p > 0.05$; interaction: $F_{1,106} = 2.497$, $p > 0.05$; data not shown). Interestingly, in this area we found a significantly enhanced age-dependent elevation of 8-hydroxyguanosine immunoreactivity in the females (sex × age interaction: $F_{1,106} = 7.222$, $p < 0.01$; Supplementary Fig. 4B). In

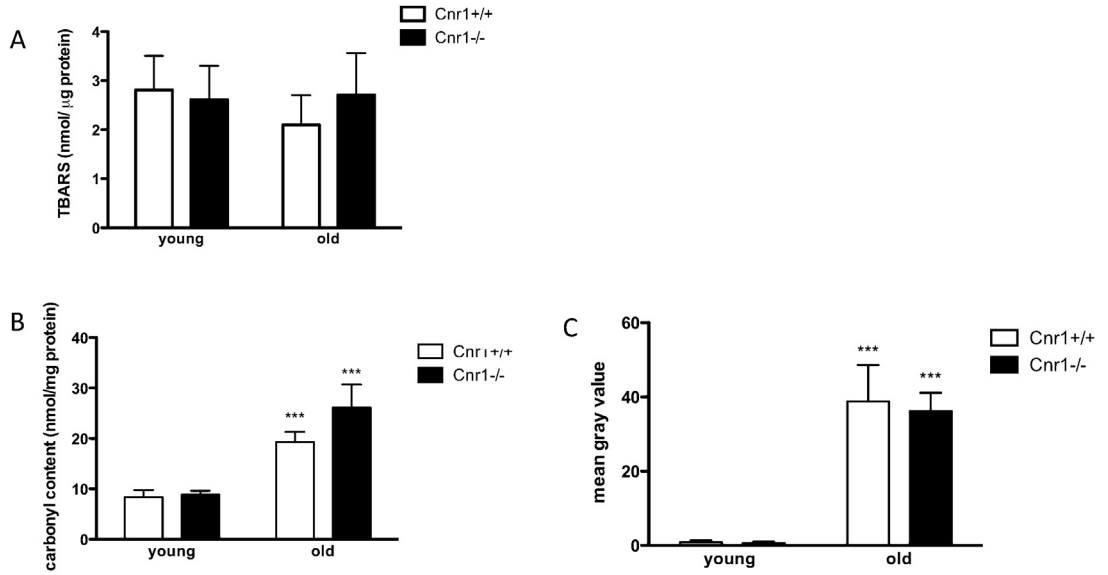

Fig. 2. Age-dependent changes in the amount of oxidized macromolecules in the hippocampus of Cnr1$^{+/+}$ and Cnr1$^{-/-}$ mice (A) No difference in lipid peroxidation measured as the concentration of thiobarbituric acid-reactive substances between age groups or genotypes (n = 4–8 per group). (B) Similar age-related increase in protein oxidation assessed as the amount of protein carbonyls in Cnr1$^{+/+}$ and Cnr1$^{-/-}$ mice (***$p < 0.001$ Bonferroni's *post hoc* test; n = 6–8 per group). (C) Age-related increase in the amount of oxidized DNA measured as 8-hydroxyguanosine staining intensity did not differ between the genotypes (***$p < 0.001$ difference between the age groups within the same genotype, Bonferroni's *post hoc* test, n = 4).

striatum, an age-related increase in 8-hydroxyguanosine levels was also recorded (age effect: $F_{1,100} = 0.468$, $p > 0.05$), but it was similar between the two genotypes and sexes (data not shown).

Supplementary material related to this article can be found, in the online version, at http://dx.doi.org/10.1016/j.mad.2013.08.001.

These results suggest that oxidative damage to proteins and DNA increases with age in the hippocampus (as well as DNA oxidation in the cortex) but this age-related change is not further exacerbated by the lack of CB1 receptors. Surprisingly, no age-related increase in lipid peroxidation was found in the brain

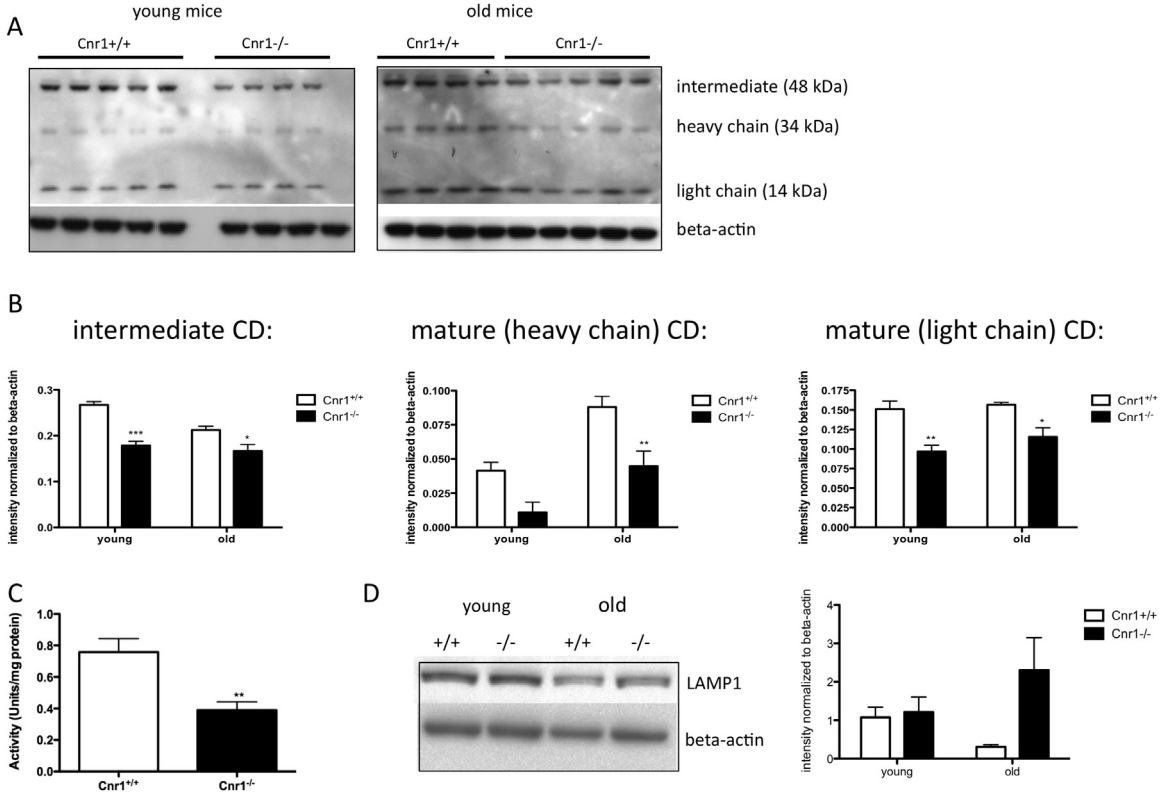

Fig. 3. Expression of lysosomal markers (cathepsin D and LAMP1) in the hippocampus of Cnr1$^{+/+}$ and Cnr1$^{-/-}$ mice (n = 4–5). (A) Representative Western blots showing the expression of different isoforms of cathepsin D in young and old Cnr1$^{+/+}$ and Cnr1$^{-/-}$ mice. (B) Densitometric analysis of Western blot data revealed decreased expression of the intermediate, 48 kDa, form and mature isoforms–heavy chain, 34 kDa, and light chain, 14 kDa, in young and old Cnr1$^{-/-}$ mice. *, **, *** indicate $p < 0.05$, $p < 0.01$, $p < 0.001$ significant difference between the genotypes using Bonferroni's *post hoc* test. (C) Cathepsin D activity is significantly reduced in the hippocampus of Cnr1$^{-/-}$ mice. ** indicate $p < 0.01$ in Student's t-test. (D) No significant difference in LAMP1 protein levels between age groups or genotypes, however, a tendency towards higher LAMP1 density in the old CB1 knockout mice could be noted (n = 4).

regions studies. Thus the enhanced accumulation of lipofuscin is not a result of higher oxidative damage in Cnr1$^{-/-}$ mice.

3.3. Loss of CB1 receptors leads to decreased levels and activity of cathepsin D, a major lysosomal protease

Since cathepsin D mutations or absence can by itself lead to exacerbated lipofuscin accumulation, we first assessed levels of different cathepsin D isoforms in the hippocampus of young and old WT and CB1 knockout mice (Fig. 3A and B).

Cathepsin D is synthesized as an inactive precursor (52 kDa) and is rapidly converted to an active 48 kDa intermediate form in endosomes, which is then further processed to a fully mature form (consistent of a 34 kDa heavy chain and a 14 kDa light chain) in the lysosomes (Masson et al., 2011). The expression of the intermediate form of cathepsin D was generally higher than that of 34 and 14 kDa chain (Fig. 3A), as previously described for mouse cells (Felbor et al., 2002; Masson et al., 2011). We found a generally reduced expression of active cathepsin D in the absence of CB1 receptor in both young and old mice (genotype effect: $F_{1,14} = 40.38$, $p < 0.001$ for the intermediate form, $F_{1,14} = 18.33$, $p < 0.001$ for the heavy chain, $F_{1,14} = 24.39$, $p < 0.001$ for the light chain; Fig. 3B). There was also an effect of age on the expression of intermediate ($F_{1,14} = 9.903$, $p < 0.01$) and heavy chain ($F_{1,14} = 21.96$, $p < 0.001$) forms. When we compared the cathepsin D activities in the hippocampus between the Cnr1$^{+/+}$ and Cnr1$^{-/-}$ mice, we found that it was significantly lower in Cnr1$^{-/-}$ mice (Fig. 3C). Additionally, we investigated a possibility that there is a general decrease in lysosomal numbers in CB1 knockout mice. In order to do so, we analysed the presence of lysosomal marker LAMP1 with Western blot (Fig. 3D). There was no significant change in the amount of LAMP1 in the CB1 knockout mice; only a slight decrease during aging in WT mice could be observed. Therefore, a decrease in CD levels does not coincide with a general decrease in lysosomal numbers.

We next assessed the possibility of different genetic regulation patterns of cathepsin D expression in the CB1 knockout mice using real-time PCR (Supplementary Fig. 5). There was a significant effect of genotype of the mRNA levels of cathepsin D (two-way ANOVA, genotype effect: $F_{1,23} = 6.475$, $p < 0.05$). The patterns of cathepsin D expression were also different during aging between the two genotypes (interaction age × genotype: $F_{1,23} = 4.896$, $p < 0.05$): the levels of cathepsin D mRNA showed no change in aging in the WT mice, but a significant decrease in cathepsin D expression was observed in the 12-month-old CB1 knockout mice.

Supplementary material related to this article can be found, in the online version, at http://dx.doi.org/10.1016/j.mad.2013.08.001.

It is known that CB1 receptor activity has an influence on ceramide levels, and ceramide is known to directly activate cathepsin D processing. Therefore, we also assessed the ceramide levels are altered in Cnr1$^{-/-}$ mice. However, neither the total ceramide level nor the ceramide profile was affected by the deletion of CB1 receptors (see Supplementary Fig. 6).

Supplementary material related to this article can be found, in the online version, at http://dx.doi.org/10.1016/j.mad.2013.08.001.

3.4. Upregulation of autophagy in old Cnr1$^{-/-}$ mice

Next, we investigated the possibility that lipofuscin accumulation in Cnr1$^{-/-}$ mice affects autophagy. Therefore, we examined the levels of autophagy markers LC3 and p62 in the hippocampus of young (2–3-month-old) and old (12–15-month-old) Cnr1$^{+/+}$ and Cnr1$^{-/-}$ mice. The accumulation of LC3-II isoform is considered to be a marker for the upregulation of autophagosomal formation. The amount of LC3-II was almost two times higher in 12-month-old Cnr1$^{-/-}$ compared to age-matched Cnr1$^{+/+}$ mice, indicating autophagy upregulation (Fig. 4A; genotype effect: $F_{1,12} = 5.73$, $p < 0.05$, interaction age x genotype: $F_{1,12} = 5.852$, $p < 0.05$). Old Cnr1$^{-/-}$ animals also had lower p62 levels as compared to Cnr1$^{+/+}$ mice (Fig. 4A; genotype effect: $F_{1,12} = 28.13$, $p < 0.001$). Lower p62 levels together with higher LC3-II synthesis could indicate enhanced autophagy in the hippocampus of old CB1 receptor deficient mice. Interestingly, there was no upregulation of LC3-II in the young Cnr1$^{-/-}$ mice (Fig. 4A) but these mice also had a lower p62 level (Fig. 4A; $p < 0.01$ in Bonferroni's *post hoc* test). This could indicate a general increase in p62 protein degradation in the absence of CB1 receptors or transcriptional regulation of p62 expression. Therefore, to clarify this question we performed real-time PCR analysis of p62/SQSTM1 expression in young and old Cnr1$^{+/+}$ and CB1 knockout mice. mRNA expression analysis has revealed that there was a significant effect of genotype on p62 expression (genotype effect: $F_{1,23} = 15.96$, $p < 0.001$) (Supplementary Fig. 7). The pattern of genetic regulation of p62 expressions seems to be quite different in the brain of two genotypes during aging (interaction age × genotype: $F_{1,23} = 7.625$, $p < 0.05$): while p62 expression was significantly lower in 12-month-old CB1 knockout mice, it increased with aging in the Cnr1$^{+/+}$ mice. The effect of age on p62 expression was not quite significant (age effect: $F_{1,23} = 3.445$, $p = 0.07$).

It is known that CB1 receptor-mediated signaling can act through the Akt/mTOR pathway (Ellert-Miklaszewska et al., 2013; Puighermanal et al., 2009) and regulate autophagy. We compared the levels of Akt and mTOR phosphorylation in young and old Cnr1$^{+/+}$ and Cnr1$^{-/-}$ mice and found no significant difference between the two strains (Supplementary Fig. 8), although mTOR phosphorylation was slightly increased in young Cnr1$^{-/-}$ mice.

Supplementary material related to this article can be found, in the online version, at http://dx.doi.org/10.1016/j.mad.2013.08.001.

3.5. Genetic deletion of CB1 receptors increases autophagic flux

To clarify the role of CB1 receptor in autophagy, we performed experiments using cultured hippocampal neurons from Cnr1$^{+/+}$ and Cnr1$^{-/-}$ mice. Neurons were treated with rapamycin (to induce autophagy) and bafiomycin A_1 (to inhibit autophagic flux) for 24 h and collected on 14DIV for p62 and LC3 analysis. The results are presented in Fig. 4B. In the absence of any treatment, neurons lacking the CB1 receptor had lower LC3-I and-II, as well as slightly, but not significantly, lower p62 levels. Rapamycin treatment had no effect on LC3-II levels, consistent with reports that it is mostly ineffective in inducing autophagy in neurons (Tsvetkov et al., 2010; Fox et al., 2010; Boland et al., 2008), however, it does lead to a decrease in p62 levels in the neurons of both genotypes, which is usually associated with autophagy upregulation. Introducing bafilomycin A_1 effectively blocked lysosomal degradation both in Cnr1$^{+/+}$ and Cnr1$^{-/-}$ neurons, as evidenced by the accumulation of LC3-II (treatment effect: $F_{2,12} = 10.74$, $p < 0.01$; Fig. 4B) and p62 (treatment effect: $F_{2,12} = 9.827$; Fig. 4B). Relative fold change in LC3-II levels after blocking the autophagic flux was significantly higher in Cnr1$^{-/-}$ neurons (Fig. 4C), indicating that autophagy rate is higher in the absence of CB1 receptors. This effect might be compensatory, since the efficiency of lysosomal degradation seems to be impaired due to low CD activity.

4. Discussion

In this study, exacerbated age-related lipofuscin accumulation was revealed in the CA3 region of the hippocampus in mice lacking CB1 receptors. Since lipofuscin accumulation can impair normal cellular functions (Kurz, 2008), and neurons cannot get rid of it by cell division, it can be detrimental for the aging brain and can contribute to cognitive impairment. CA3 region of the hippocampus

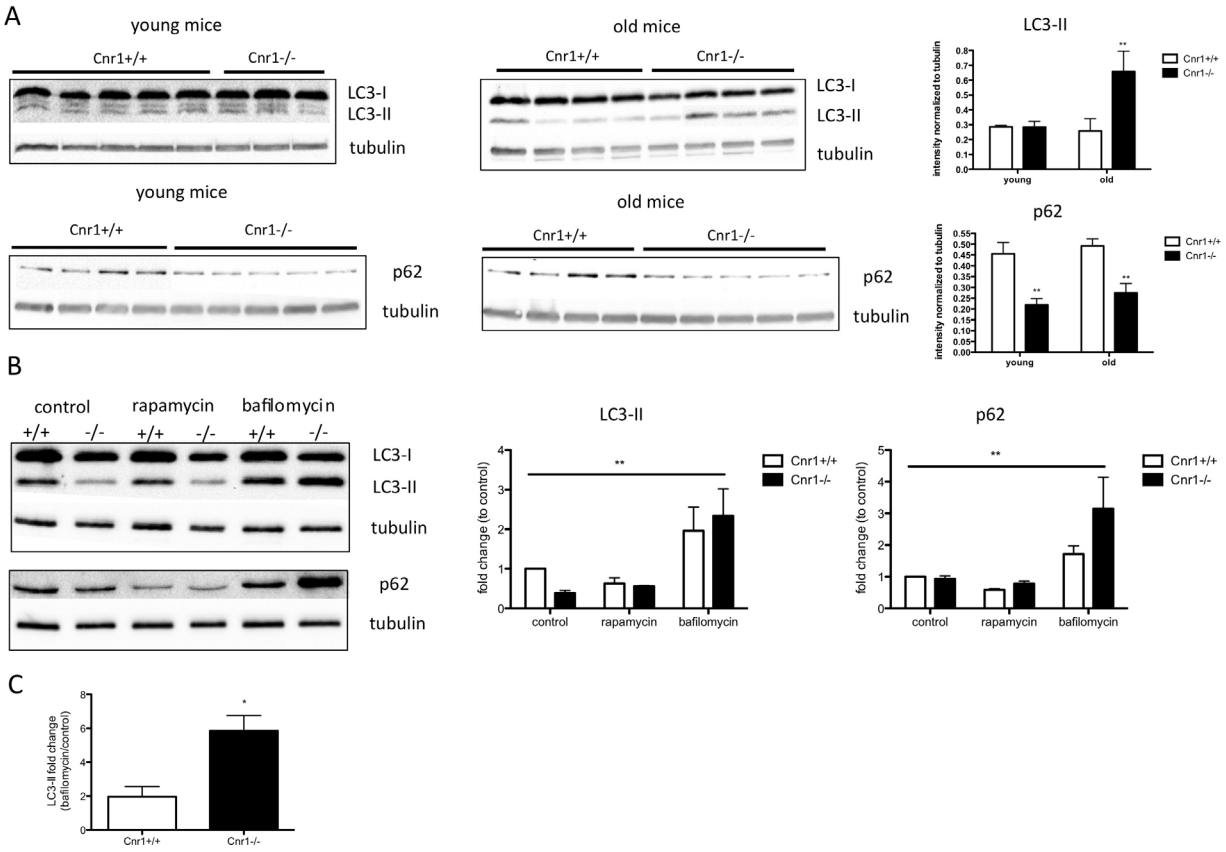

Fig. 4. Autophagic markers (LC3, p62) in the hippocampus of $Cnr1^{+/+}$ and $Cnr1^{-/-}$ mice (A) and measurements of autophagic flux in hippocampal neurons (B and C). (A) Lipidation of LC3 (LC3-II level) was increased in 12-month-old $Cnr1^{-/-}$ mice (*$p < 0.05$ in Bonferroni's *post hoc* test; $n = 3–5$). $Cnr1^{-/-}$ animals had lower p62 levels in the hippocampus compared to $Cnr1^{+/+}$ mice (**$p < 0.01$ significant difference between the genotypes within the same age-group using Bonferroni's *post hoc* test; $n = 4–5$). (B) Western blot analysis of autophagic markers in hippocampal neurons from $Cnr1^{+/+}$ and $Cnr1^{-/-}$ mice ($n = 3$). Basal level of LC3-II was lower in $Cnr1^{-/-}$ hippocampal neurons. There was no effect of rapamycin treatment on LC3-II levels, but the level of p62 was slightly decreased. Treatment with bafilomycin (20 nM) resulted in a significant increase in LC3-II and p62 levels in both $Cnr1^{+/+}$ and $Cnr1^{-/-}$ neurons, indicating the block of autophagic flux. **$p < 0.01$ treatment effect (two-way ANOVA). (C) Autophagic flux is significantly upregulated in the absence of CB1 receptors. LC3-II accumulation after bafilomycin treatment in comparison to basal levels was calculated for $Cnr1^{+/+}$ and $Cnr1^{-/-}$ neurons. Fold increase in LC3-II levels after the treatment was significantly higher in the absence of CB1 receptors, indicating higher autophagy rate (*$p < 0.05$, unpaired *t*-test).

plays a unique role in spatial learning (Kesner, 2007), and age-related lesions in the CA3 region (lipofuscin accumulation and neuronal loss) have been correlated to memory impairment in 12-month-old rats (Kadar et al., 1990). Therefore, increased accumulation of lipofuscin selectively in this region can contribute to the impaired learning and memory abilities of 12-month-old $Cnr1^{-/-}$ mice (Albayram et al., 2011, 2012).

Lipofuscin accumulation in the hippocampus has been linked to age-related oxidative stress (Assuncao et al., 2011). Therefore, we first considered that the elevated lipofuscin load in the $Cnr1^{-/-}$ mice could be a result of increased production of oxidized macromolecules. However, the age-related increase in the amount of oxidized proteins and DNA was comparable between the genotypes.

Although lipofuscin accumulation can result from oxidative stress, studies have shown that these two processes do not always correlate with each other (Hutter et al., 2007). Therefore, we next asked, whether impaired clearance of degradation products is responsible for the observed phenotype of $Cnr1^{-/-}$ animals. It is known that the knockout of cathepsin D, one of the major lysosomal proteases, causes symptoms similar to those in neuronal ceroid lipofuscinosis characterized by a massive accumulation of autofluorescent ceroid/lipofuscin in the CNS neurons and cognitive deficits (Koike et al., 2000; Nakanishi et al., 2001). Therefore, a decrease in cathepsin D activity can contribute to the enhanced lipofuscin accumulation due to the impaired clearance of damaged macromolecules. We compared cathepsin D expression in $Cnr1^{+/+}$ and $Cnr1^{-/-}$ mice and found that $Cnr1^{-/-}$ mice had decreased cathepsin D expression in the hippocampus. The activity of cathepsin D was also significantly lower in the absence of CB1 receptors. This could have a direct effect on lysosomal function and account for higher lipofuscin accumulation in the CB1 knockout animals. Few studies have addressed the role of CB1 receptors in the lysosome so far. For instance, it has been shown that the majority of CB1 receptors in the cell are present in lysosomes and late endosomes (Rozenfeld and Devi, 2008). Treatment of cells with CB1 receptor agonist Δ^9-THC also affects lysosomal integrity (Gowran and Campbell, 2008). However, the role of CB1 receptors on lysosomes is not clear yet. It has been shown recently that these CB1 receptors can be activated by endogenous cannabinoids (Brailoiu et al., 2011); therefore, they are functional and can play a physiologically relevant role. The results of this study indicate that the presence of functional CB1 receptors is important for the regulation of cathepsin D expression and activity. One of the possibilities could be transcriptional control of cathepsin D expression. Indeed, we observe a significant effect of CB1 receptor presence on the expression of cathepsin D mRNA, especially in old animals. However, it does not quite explain the low protein levels of cathepsin D in young CB1 knockout mice. This suggests that there are other mechanisms that influence cathepsin D levels in the CB1 knockout mice. It is also known that CB1 receptor activation can induce ceramide synthesis (Velasco et al., 2005), and ceramide

can directly activate cathepsin D (Heinrich et al., 1999). Therefore, absence of CB1 receptor activity can indirectly influence cathepsin D activation by affecting ceramide synthesis. However, neither the total ceramide levels nor the ceramide profile differed between the $Cnr1^{+/+}$ and $Cnr1^{-/-}$ mice (see Supplementary Fig. 6). Therefore, an indirect regulation of cathepsin D expression through ceramide is rather improbable.

Accumulation of lipofuscin is also attributed to deficits in autophagy. Lipofuscin can prevent fusion of lysosomes with autophagosomes, leading to accumulation of autophagosomes, which was reported for a knockout mouse model of juvenile neuronal lipofuscinosis (Cao et al., 2006). Therefore, we investigated the presence of autophagy markers (p62, LC3) in the hippocampus of $Cnr1^{+/+}$ and $Cnr1^{-/-}$ mice. In young mice, the levels of lipidated form of LC3, LC3-II, which is associated with the autophagosomal membrane, were not changed in the absence of CB1 receptor. However, LC3-II was significantly upregulated in the hippocampus of old $Cnr1^{-/-}$ mice, and the conversion of LC3-I to LC3-II (LC3-II/I ratio) was also higher in the knockout strain (data not shown), indicating an increase in autophagosome formation. It has been shown that lipofuscin can be loaded into the lysosomes *via* autophagy (Hohn et al., 2012) to prevent oxidative damage in the cytosol. Therefore, increased formation of autophagosomes could serve as a compensatory mechanism. However, since the levels of active cathepsin D are decreased upon CB1 receptor absence, this compensation cannot lead to a decrease in lipofuscin levels, but might explain why there was no general increase in oxidative stress in the knockout strain despite of lipofuscin accumulation.

The p62 protein is known to be a substrate of autophagy and its levels are often related to autophagy function (Mizushima et al., 2010). The levels of p62 are decreased in both old and young CB1 knockout mice, as indicated by Western blot analysis. However, p62 can be transcriptionally regulated during autophagy and can also serve as a substrate for different degradation pathways, which confounds the interpretation of this result. To test the possibility of transcriptional regulation of p62 upon CB1 receptor deletion, we performed real-time PCR analysis using RNA isolated from young and old WT and CB1 knockout mice hippocampi. The expression of p62 mRNA was significantly decreased in the old CB1 knockout mice. The downregulation of p62 found in the absence of CB1 receptors at both protein and mRNA levels, therefore, could be partially related to autophagy upregulation, but also to a down-regulation of p62 expression.

Studies of autophagy in hippocampal neurons from $Cnr1^{+/+}$ and $Cnr1^{-/-}$ mice indicate that autophagic flux is increased in the cells lacking CB1 receptors. Blocking lysosomal degradation *via* bafilomycin A_1 lead to a much higher accumulation of LC3-II levels in $Cnr1^{-/-}$ neurons, as compared to basal levels, indicating that the absence of CB1 receptors leads to faster turnover of autophagosomes in neurons. This effect can have at least two possible explanations. Upregulation of autophagic flux can be compensatory and serve to partially counteract the decreased lysosomal degradative capacity due to low cathepsin D activity. Alternatively, the lack of CB1 receptors by itself can lead to alterations in the autophagic process. The latter possibility seems counterintuitive since several studies have shown that the activation of CB1 receptors, at least in cancer cells, leads to autophagy upregulation (Donadelli et al., 2011; Ellert-Miklaszewska et al., 2013; Salazar et al., 2009; Vara et al., 2011).

In summary, we could show that the lack of CB1 receptors leads to exacerbated accumulation of aging pigment lipofuscin specifically in the CA3 region of the hippocampus but not in other brain regions. We propose that decreased expression of cathepsin D together with a general increase in oxidative stress during aging contribute to exacerbated lipofuscin accumulation in the aged CB1 knockout mice. Although a decrease in active cathepsin D levels is also present in young $Cnr1^{-/-}$ mice, the impact of impaired lysosomal function on macromolecule clearance increases in aging. Therefore, low CB1 receptor activity in aging may lead to increased accumulation and impaired clearance of damaged macromolecules, which in turn can cause neuronal loss and increased neuroinflammation.

Acknowledgements

We would like to thank Dr. Daniele Bano for his helpful comments on the manuscript. We also thank Prof. Dr. Andreas Zimmer for providing CB1 knockout mice and discussion of the results. This work was supported by a grant (FOR926-SP2) of the German Research Council (DFG). All authors declare that they have no actual or potential conflicts of interest.

References

Albayram, O., Alferink, J., Pitsch, J., Piyanova, A., Neitzert, K., Poppensieker, K., Mauer, D., Michel, K., Legler, A., Becker, A., Monory, K., Lutz, B., Zimmer, A., Bilkei-Gorzo, A., 2011. Role of CB1 cannabinoid receptors on GABAergic neurons in brain aging. Proc. Natl. Acad. Sci. U.S.A. 108, 11256–11261.

Albayram, O., Bilkei-Gorzo, A., Zimmer, A., 2012. Loss of CB1 receptors leads to differential age-related changes in reward-driven learning and memory. Front Aging Neurosci. 4, 34.

Assuncao, M., Santos-Marques, M.J., Carvalho, F., Lukoyanov, N.V., Andrade, J.P., 2011. Chronic green tea consumption prevents age-related changes in rat hippocampal formation. Neurobiol. Aging 32, 707–717.

Bilkei-Gorzo, A., Drews, E., Albayram, O., Piyanova, A., Gaffal, E., Tueting, T., Michel, K., Mauer, D., Maier, W., Zimmer, A., 2012. Early onset of aging-like changes is restricted to cognitive abilities and skin structure in Cnr1(−/−) mice. Neurobiol. Aging 33 , 200.e211–222.

Bilkei-Gorzo, A., Racz, I., Valverde, O., Otto, M., Michel, K., Sastre, M., Zimmer, A., 2005. Early age-related cognitive impairment in mice lacking cannabinoid CB1 receptors. Proc. Natl. Acad. Sci. U.S.A. 102, 15670–15675.

Bishop, N.A., Lu, T., Yankner, B.A., 2010. Neural mechanisms of ageing and cognitive decline. Nature 464, 529–535.

Boland, B., Kumar, A., Lee, S., Platt, F.M., Wegiel, J., Yu, W.H., Nixon, R.A., 2008. Autophagy induction and autophagosome clearance in neurons: relationship to autophagic pathology in Alzheimer's disease. J. Neurosci. 28, 6926–6937.

Brailoiu, G.C., Oprea, T.I., Zhao, P., Abood, M.E., Brailoiu, E., 2011. Intracellular cannabinoid type 1 (CB1) receptors are activated by anandamide. J. Biol. Chem. 286, 29166–29174.

Bruce, A.J., Baudry, M., 1995. Oxygen free radicals in rat limbic structures after kainate-induced seizures. Free Radic. Biol. Med. 18, 993–1002.

Brunk, U.T., Terman, A., 2002. The mitochondrial-lysosomal axis theory of aging: accumulation of damaged mitochondria as a result of imperfect autophagocytosis. Eur. J. Biochem. 269, 1996–2002.

Cai, J., Qi, X., Kociok, N., Skosyrski, S., Emilio, A., Ruan, Q., Han, S., Liu, L., Chen, Z., Bowes Rickman, C., Golde, T., Grant, M.B., Saftig, P., Serneels, L., de Strooper, B., Joussen, A.M., Boulton, M.E., 2012. beta-Secretase (BACE1) inhibition causes retinal pathology by vascular dysregulation and accumulation of age pigment. EMBO Mol. Med. 4, 980–991.

Cao, Y., Espinola, J.A., Fossale, E., Massey, A.C., Cuervo, A.M., MacDonald, M.E., Cotman, S.L., 2006. Autophagy is disrupted in a knock-in mouse model of juvenile neuronal ceroid lipofuscinosis. J. Biol. Chem. 281, 20483–20493.

Di Marzo, V., Bifulco, M., De Petrocellis, L., 2004. The endocannabinoid system and its therapeutic exploitation. Nat. Rev. Drug Discov. 3, 771–784.

Donadelli, M., Dando, I., Zaniboni, T., Costanzo, C., Dalla Pozza, E., Scupoli, M.T., Scarpa, A., Zappavigna, S., Marra, M., Abbruzzese, A., Bifulco, M., Caraglia, M., Palmieri, M., 2011. Gemcitabine/cannabinoid combination triggers autophagy in pancreatic cancer cells through a ROS-mediated mechanism. Cell Death Dis. 2, e152.

Dubey, A., Forster, M.J., Lal, H., Sohal, R.S., 1996. Effect of age and caloric intake on protein oxidation in different brain regions and on behavioral functions of the mouse. Arch. Biochem. Biophys. 333, 189–197.

Dunlop, R.A., Brunk, U.T., Rodgers, K.J., 2009. Oxidized proteins: mechanisms of removal and consequences of accumulation. IUBMB Life 61, 522–527.

Ellert-Miklaszewska, A., Ciechomska, I., Kaminska, B., 2013. Cannabinoid signaling in glioma cells. Adv. Exp. Med. Biol. 986, 209–220.

Farwanah, H., Kolter, T., Sandhoff, K., 2011. Mass spectrometric analysis of neutral sphingolipids: methods, applications, and limitations. Biochim. Biophys. Acta.

Farwanah, H., Wirtz, J., Kolter, T., Raith, K., Neubert, R.H., Sandhoff, K., 2009. Normal phase liquid chromatography coupled to quadrupole time of flight atmospheric pressure chemical ionization mass spectrometry for separation, detection and mass spectrometric profiling of neutral sphingolipids and cholesterol. J. Chromatogr. B: Analyt. Technol. Biomed. Life Sci. 877, 2976–2982.

Felbor, U., Kessler, B., Mothes, W., Goebel, H.H., Ploegh, H.L., Bronson, R.T., Olsen, B.R., 2002. Neuronal loss and brain atrophy in mice lacking cathepsins B and L. Proc. Natl. Acad. Sci. U.S.A. 99, 7883–7888.

Fox, J.H., Connor, T., Chopra, V., Dorsey, K., Kama, J.A., Bleckmann, D., Betschart, C., Hoyer, D., Frentzel, S., Difiglia, M., Paganetti, P., Hersch, S.M., 2010. The mTOR kinase inhibitor Everolimus decreases S6 kinase phosphorylation but fails to reduce mutant huntingtin levels in brain and is not neuroprotective in the R6/2 mouse model of Huntington's disease. Mol. Neurodegen. 5, 26.

Golden, T.R., Hinerfeld, D.A., Melov, S., 2002. Oxidative stress and aging: beyond correlation. Aging Cell 1, 117–123.

Gowran, A., Campbell, V.A., 2008. A role for p53 in the regulation of lysosomal permeability by delta 9-tetrahydrocannabinol in rat cortical neurones: implications for neurodegeneration. J. Neurochem. 105, 1513–1524.

Harman, D., 1956. Aging: a theory based on free radical and radiation chemistry. J. Gerontol. 11, 298–300.

Heinrich, M., Wickel, M., Schneider-Brachert, W., Sandberg, C., Gahr, J., Schwandner, R., Weber, T., Saftig, P., Peters, C., Brunner, J., Kronke, M., Schutze, S., 1999. Cathepsin D targeted by acid sphingomyelinase-derived ceramide. EMBO J. 18, 5252–5263.

Hekimi, S., Guarente, L., 2003. Genetics and the specificity of the aging process. Science 299, 1351–1354.

Hohn, A., Jung, T., Grimm, S., Grune, T., 2010. Lipofuscin-bound iron is a major intracellular source of oxidants: role in senescent cells. Free Radic. Biol. Med. 48, 1100–1108.

Hohn, A., Sittig, A., Jung, T., Grimm, S., Grune, T., 2012. Lipofuscin is formed independently of macroautophagy and lysosomal activity in stress-induced prematurely senescent human fibroblasts. Free Radic. Biol. Med. 53, 1760–1769.

Hutter, E., Skovbro, M., Lener, B., Prats, C., Rabol, R., Dela, F., Jansen-Durr, P., 2007. Oxidative stress and mitochondrial impairment can be separated from lipofuscin accumulation in aged human skeletal muscle. Aging Cell 6, 245–256.

Kadar, T., Silbermann, M., Brandeis, R., Levy, A., 1990. Age-related structural changes in the rat hippocampus: correlation with working memory deficiency. Brain Res. 512, 113–120.

Kesner, R.P., 2007. Behavioral functions of the CA3 subregion of the hippocampus. Learn. Mem. 14, 771–781.

Kim, S.H., Won, S.J., Mao, X.O., Jin, K., Greenberg, D.A., 2005. Involvement of protein kinase A in cannabinoid receptor-mediated protection from oxidative neuronal injury. J. Pharmacol. Exp. Ther. 313, 88–94.

Koike, M., Nakanishi, H., Saftig, P., Ezaki, J., Isahara, K., Ohsawa, Y., Schulz-Schaeffer, W., Watanabe, T., Waguri, S., Kametaka, S., Shibata, M., Yamamoto, K., Kominami, E., Peters, C., von Figura, K., Uchiyama, Y., 2000. Cathepsin D deficiency induces lysosomal storage with ceroid lipofuscin in mouse CNS neurons. J. Neurosci. 20, 6898–6906.

Kurz, T., 2008. Can lipofuscin accumulation be prevented? Rejuvenation Res. 11, 441–443.

Levine, R.L., 2002. Carbonyl modified proteins in cellular regulation, aging, and disease. Free Radic. Biol. Med. 32, 790–796.

Levine, R.L., Williams, J.A., Stadtman, E.R., Shacter, E., 1994. Carbonyl assays for determination of oxidatively modified proteins. Methods Enzymol. 233, 346–357.

Livak, K.J., Schmittgen, T.D., 2001. Analysis of relative gene expression data using real-time quantitative PCR and the 2(-Delta Delta C(T)) method. Methods 25, 402–408.

Lutz, B., 2002. Molecular biology of cannabinoid receptors. Prostaglandins Leukot. Essent. Fatty Acids 66, 123–142.

Ma, W., Coon, S., Zhao, L., Fariss, R.N., Wong, W.T., 2013. A2E accumulation influences retinal microglial activation and complement regulation. Neurobiol. Aging 34, 943–960.

Masson, O., Prebois, C., Derocq, D., Meulle, A., Dray, C., Daviaud, D., Quilliot, D., Valet, P., Muller, C., Liaudet-Coopman, E., 2011. Cathepsin-D, a key protease in breast cancer, is up-regulated in obese mouse and human adipose tissue, and controls adipogenesis. PLoS ONE 6, e16452.

Mizushima, N., Yoshimori, T., Levine, B., 2010. Methods in mammalian autophagy research. Cell 140, 313–326.

Nakanishi, H., 2003. Neuronal and microglial cathepsins in aging and age-related diseases. Ageing Res. Rev. 2, 367–381.

Nakanishi, H., Amano, T., Sastradipura, D.F., Yoshimine, Y., Tsukuba, T., Tanabe, K., Hirotsu, I., Ohono, T., Yamamoto, K., 1997. Increased expression of cathepsins E and D in neurons of the aged rat brain and their colocalization with lipofuscin and carboxy-terminal fragments of Alzheimer amyloid precursor protein. J. Neurochem. 68, 739–749.

Nakanishi, H., Zhang, J., Koike, M., Nishioku, T., Okamoto, Y., Kominami, E., von Figura, K., Peters, C., Yamamoto, K., Saftig, P., Uchiyama, Y., 2001. Involvement of nitric oxide released from microglia-macrophages in pathological changes of cathepsin D-deficient mice. J. Neurosci. 21, 7526–7533.

Paxinos, G., Franklin, K., 2001. The Mouse Brain in Stereotaxic Coordinates. Academic Press, London, UK.

Puighermanal, E., Marsicano, G., Busquets-Garcia, A., Lutz, B., Maldonado, R., Ozaita, A., 2009. Cannabinoid modulation of hippocampal long-term memory is mediated by mTOR signaling. Nat. Neurosci. 12, 1152–1158.

Reznick, A.Z., Packer, L., 1994. Oxidative damage to proteins: spectrophotometric method for carbonyl assay. Methods Enzymol. 233, 357–363.

Rozenfeld, R., Devi, L.A., 2008. Regulation of CB1 cannabinoid receptor trafficking by the adaptor protein AP-3. FASEB J. 22, 2311–2322.

Salazar, M., Carracedo, A., Salanueva, I.J., Hernandez-Tiedra, S., Lorente, M., Egia, A., Vazquez, P., Blazquez, C., Torres, S., Garcia, S., Nowak, J., Fimia, G.M., Piacentini, M., Cecconi, F., Pandolfi, P.P., Gonzalez-Feria, L., Iovanna, J.L., Guzman, M., Boya, P., Velasco, G., 2009. Cannabinoid action induces autophagy-mediated cell death through stimulation of ER stress in human glioma cells. J. Clin. Invest. 119, 1359–1372.

Sastre, J., Pallardo, F.V., Vina, J., 2003. The role of mitochondrial oxidative stress in aging. Free Radic. Biol. Med. 35, 1–8.

Shiozaki, M., Yoshimura, K., Shibata, M., Koike, M., Matsuura, N., Uchiyama, Y., Gotow, T., 2008. Morphological and biochemical signs of age-related neurodegenerative changes in klotho mutant mice. Neuroscience 152, 924–941.

Strazielle, C., Jazi, R., Verdier, Y., Qian, S., Lalonde, R., 2009. Regional brain metabolism with cytochrome c oxidase histochemistry in a PS1/A246E mouse model of autosomal dominant Alzheimer's disease: correlations with behavior and oxidative stress. Neurochem. Int. 55, 806–814.

Terman, A., Brunk, U.T., 2004. Lipofuscin. Int. J. Biochem. Cell Biol. 36, 1400–1404.

Tsvetkov, A.S., Miller, J., Arrasate, M., Wong, J.S., Pleiss, M.A., Finkbeiner, S., 2010. A small-molecule scaffold induces autophagy in primary neurons and protects against toxicity in a Huntington disease model. Proc. Natl. Acad. Sci. U.S.A. 107, 16982–16987.

Vara, D., Salazar, M., Olea-Herrero, N., Guzman, M., Velasco, G., Diaz-Laviada, I., 2011. Anti-tumoral action of cannabinoids on hepatocellular carcinoma: role of AMPK-dependent activation of autophagy. Cell Death Differ. 18, 1099–1111.

Velasco, G., Galve-Roperh, I., Sanchez, C., Blazquez, C., Haro, A., Guzman, M., 2005. Cannabinoids and ceramide: two lipids acting hand-by-hand. Life Sci. 77, 1723–1731.

Walls, K.C., Klocke, B.J., Saftig, P., Shibata, M., Uchiyama, Y., Roth, K.A., Shacka, J.J., 2007. Altered regulation of phosphatidylinositol 3-kinase signaling in cathepsin D-deficient brain. Autophagy 3, 222–229.

Yamasaki, R., Zhang, J., Koshiishi, I., Sastradipura Suniarti, D.F., Wu, Z., Peters, C., Schwake, M., Uchiyama, Y., Kira, J., Saftig, P., Utsumi, H., Nakanishi, H., 2007. Involvement of lysosomal storage-induced p38 MAP kinase activation in the overproduction of nitric oxide by microglia in cathepsin D-deficient mice. Mol. Cell. Neurosci. 35, 573–584.